Published in final edited form as:
J Neurosurg. 2008 November ; 109(5): 874–880. doi:10.3171/JNS/2008/109/11/0874.

Detection of infusate leakage in the brain using real-time imaging of convection-enhanced delivery:

Laboratory investigation

Vanja Varenika, B.S.[1], **Peter Dickinson, B.V.Sc., Ph.D.**[2], **John Bringas, B.S.**[1], **Richard LeCouteur, B.V.Sc., Ph.D.**[2], **Robert Higgins, D.V.M., Ph.D.**[2], **John Park, M.D.**[1], **Massimo Fiandaca, M.D.**[1,3], **Mitchel Berger, M.D.**[1], **John Sampson, M.D., Ph.D.**[4], and **Krystof Bankiewicz, M.D., Ph.D.**[1]

[1]Department of Neurological Surgery, University of California, San Francisco [2]Department of Surgical and Radiological Sciences, University of California, Davis, School of Veterinary Medicine, Davis, California [3]Department of Neurosurgery, LifeBridge Health Brain & Spine Institute, Baltimore, Maryland [4]Division of Neurosurgery, Duke University Medical Center, Durham, North Carolina

Abstract

Object—The authors have shown that convection-enhanced delivery (CED) of gadoteridol-loaded liposomes (GDLs) into different regions of normal monkey brain results in predictable, widespread distribution of this tracking agent as detected by real-time MR imaging. They also have found that this tracking technique allows monitoring of the distribution of similar nanosized agents such as therapeutic liposomes and viral vectors. A limitation of this procedure is the unexpected leakage of liposomes out of targeted parenchyma or malignancies into sulci and ventricles. The aim of the present study was to evaluate the efficacy of CED after the onset of these types of leakage.

Methods—The authors documented this phenomenon in a study of 5 nonhuman primates and 7 canines, comprising 54 CED infusion sessions. Approximately 20% of these infusions resulted in leakage into cerebral ventricles or sulci. All of the infusions and leakage events were monitored with real-time MR imaging. The authors created volume-distributed versus volume-infused graphs for each infusion session. These graphs revealed the rate of distribution of GDL over the course of each infusion and allowed the authors to evaluate the progress of CED before and after leakage.

Results—The distribution of therapeutics within the target structure ceased to increase or resulted in significant attenuation after the onset of leakage.

Conclusions—An analysis of the cases in this study revealed that leakage undermines the efficacy of CED. These findings reiterate the importance of real-time MR imaging visualization during CED to ensure an accurate, robust distribution of therapeutic agents.

Keywords

brain; convection-enhanced delivery; leakage; liposome; magnetic resonance imaging; real-time imaging

Delivering drugs effectively to the central nervous system has always presented a challenge. The blood–brain barrier prevents significant amounts of systemically administered agents from

Address correspondence to: Krystof Bankiewicz, M.D., Ph.D., 1855 Folsom Street, Room 226, San Francisco, California 94103. Krystof.Bankiewicz@ucsf.edu.

reaching the brain. Advances in pharmacology, such as manipulation by drugs of capillary permeability, have only enabled < 1% of systemically administered drugs to pass through the blood–brain barrier.[7,26,27] To achieve therapeutic concentrations of a drug within the interstitium of the brain, extremely high systemic doses are needed, which normally result in unacceptable toxicities. Traditional local delivery of most therapeutic agents into the brain (for example, biodegradable polymers and cerebroventricular injections) has relied on diffusion, which is dependent on a concentration gradient. The rate of diffusion is inversely proportional to the size of the agent and is usually slow with respect to tissue clearance; thus, diffusion results in a nonhomogeneous distribution of most agents and is restricted to a few millimeters from the source. In contrast to diffusion, CED uses a pressure gradient established at the tip of an infusion catheter to create bulk flow, which "pushes" the drug throughout the extracellular space.[2] This displacement allows the infused material to engage the vasculature, and the rhythmic contractions of blood vessels act as an efficient motive force to move particles along perivascular tracts.[6] As a result, a higher concentration of drug is distributed more evenly and over a larger volume than by diffusion alone. Convection-enhanced delivery requires accurate placement of catheters in the brain for microinfusion of the drug, making the technique a precise system for drug administration. Currently, this delivery method is clinically used in the fields of neurooncology[12,18] and neurodegenerative diseases[5,22] such as Parkinson disease.

The volume of distribution for a given agent depends on the structural properties of tissue such as hydraulic conductivity, vascular volume fraction, and extracellular fluid fraction. It also depends on parameters of the infusion procedure such as cannula placement, cannula design, and infusion rate. To maximize delivery and minimize reflux, the infusion procedure must be adjusted according to tissue properties. We have shown that CED can homogeneously distribute large therapeutic molecules over considerable distances. Convection has also shown enhanced distribution of high-molecular-weight molecules in the normal rat, cat, and nonhuman primate brain by an order of magnitude relative to diffusion.[1,4,15,19] Based on our experience, CED allows significant infusion of therapeutic macromolecules and small viral constructs such as the adenoassociated virus into subcortical regions of the nonhuman primate brain.[1,15] In a direct comparison of CED and simple injection of adenoassociated virus in monkeys, we found a significant increase in gene transfer by using the CED method. These results indicate that efficient gene delivery can be translated to the size of a human brain.

In our opinion, one of the key components of a direct delivery system such as CED is real-time imaging. Visualizing infused drug distribution is necessary to ensure accurate delivery of therapeutic agents into target sites while minimizing exposure of healthy tissue. In vivo imaging allows active feedback on cannula placement and real-time control of drug delivery. Currently, there are several visualization systems that can track infused agents. The T2-weighted MR imaging procedure can indirectly monitor drug distribution by its effects on targeted tissue[17] and the enhancement of signal due to fluid administration. Single-photon emission computed tomography has also been used to track surrogate tracers such a radioactive iodine-123 conjugated with albumin.[25] We have developed an MR imaging–based method to visualize the distribution achieved via CED by coconvecting GDLs with therapeutic agents.[10,11,23] This method has given us the ability to directly monitor the local delivery of therapeutic agents and has improved the efficacy of CED in animals with spontaneously developed brain tumors.

Monitoring the progress of infusions in real-time has revealed that the leakage of therapeutic agents out of brain parenchyma is surprisingly common. As we describe in this report, ~ 20% of our infusions resulted in leakage into ventricles and sulci. These leaks occurred in the middle of the infusion sessions, after the placement of cannulas and the initiation of drug delivery. The leakage of therapeutic agents is a cause for concern as it can undermine the efficacy of the CED infusion. Additionally, it can cause toxicity due to flow into the CSF and exposure of re mote regions of the brain. This concern is significant when delivering viral vectors, which have

the potential to transduce untargeted cells. We studied each instance of leak age and sought to define the effects on the volume of distribution of the therapeutic agents. Although we do not pro pose to fully explore the mechanisms of leakage in the cases in the present study, we do show that leakage occurs even in experienced hands and needs to be visualized to adequately adjust treatment. This analysis may help a neurosurgeon decide the best course of action to take at the onset of such leakages. Our results may also explain some of the failures of CED in clinical trials, as many investigators have not visualized the infusions and therefore would not have noticed spontaneous leakages.[9,12,13]

Methods

Liposome Preparation

Liposomes containing an MR imaging contrast agent were composed of DOPC/cholesterol/PEG-DSG with a molar ratio of 3:2:0.3. The DOPC was purchased from Avanti Polar Lipids, the PEG-DSG from the NOF Corp., and the cholesterol from Calbiochem/EMD Chemicals Inc. Lipids were dissolved in chloroform/methanol (90:10 vol/vol), and the solvent was removed by rotary evaporation, resulting in a thin lipid film. The lipid film was dissolved in ethanol and heated to 60°C. A commercial US Pharmacopoeia solution of 0.5 M gadoteridol (ProHance, Bracco Diagnostics, Inc.) was heated to 60°C and rapidly injected into the ethanol/lipid solution. Unilamellar liposomes were formed by extrusion (Lipex, Northern Lipids Inc.) with 15 passes through double-stacked polycarbonate membranes (Whatman Nucleopore) with a pore size of 100 nm, resulting in a liposome diameter of 124 ± 24.4 nm as determined by quasielastic light scattering (N4Plus particle size analyzer, Beckman Coulter). Unencapsulated gadoteridol was removed with a Sephadex G-75 (Sigma-Aldrich) size-exclusion column eluted with HEPES-buffered saline (5 mM HEPES, 135 mM NaCl, pH 6.5, adjusted with NaOH).

Quantitation of Liposome-Entrapped Gadoteridol by MR Imaging

The concentration of gadoteridol entrapped in the liposomes was determined from nuclear MR relaxivity measurements. The relationship between the change in the intrinsic relaxation rate imposed by a paramagnetic agent (ΔR), also known as "T1 shortening," and the concentration of the agent was defined by the equation, $\Delta R = r_1[\text{agent}]$, in which r_1 = relaxivity of the paramagnetic agent and $\Delta R = (1/T1_{\text{observed}} - 1/T1_{\text{intrinsic}})$. As gadoteridol was encapsulated within the liposome, we corrected for the change in the observed T1 imposed by the lipid by the measurement of the T1 of solubilized liposomes, with and without gadoteridol, using an iterative inversion recovery MR imaging sequence on a 2-T Brucker Omega unit (Brucker Medical). The relaxivity of gadoteridol had been empirically derived on the same system and had a value of 4.07 $mM^{-1}sec^{-1}$. The concentration of the encapsulated gadoteridol was then calculated with the following equation: $[\text{gadoteridol}] = [(1/T1_{\text{w/Gado}}) - (1/T1_{\text{w/oGado}})]/4.07$.

Liposome Infusion in Nonhuman Primates

The protocol was reviewed and approved by the Institutional Animal Care and Use Committees at the University of California, San Francisco. Five adult male cynomolgus monkeys *(Macaca fascicularis)* weighing 3–10 kg were individually housed in stainless steel cages. Each animal room was maintained on a 12-hour light/dark cycle, and the room temperature ranged from 64°F to 84°F. Purina Primate Diet was provided on a daily basis in amounts appropriate for the size and age of the animals. This diet was supplemented with fruit or vegetables daily. In addition, small bits of fruit, cereal, or other treats were provided as part of the environmental enrichment program. Tap water was freely available to each animal through an automatic watering device or an attached water bottle. Prior to assignment to the study, all imported animals underwent a quarantine period of at least 31 days, as mandated by the Centers for Disease Control and Prevention.

A baseline MR image was obtained in each of the animals, who underwent neurosurgical procedures to position an MR imaging–compatible guide cannula within specific regions of the brain (for example, the putamen and corona radiata). Each guide cannula was specifically customized for the procedure and stereotactically guided to reach its target through a bur hole created in the skull. Each guide cannula was secured to the skull with dental acrylic, and the tops of the guide cannula assemblies were capped with stylet screws for simple access during the infusion procedure. Animals recovered for at least 2 weeks before initiation of the liposome infusions. During each liposome-enhanced infusion procedure, the animal was anesthetized with isoflurane, the head was placed in an MR imaging–compatible stereotactic frame, and baseline MR imaging was performed. Vital signs, such as heart rate and PO_2, were monitored throughout the procedure. Infusions were performed according to previously established CED techniques for nonhuman primates.[1] Briefly, the infusion system consisted of a fused-silica needle cannula that was connected to a loading line (containing liposomes) and an oil-infusion line. A 1-ml syringe (filled with oil), mounted onto a microinfusion pump (BeeHive, Bioanalytical Systems), regulated the flow of fluid through the system. Based on MR imaging coordinates, the cannula was mounted on to a stereotactic holder and manually guided to the targeted regions of the brain through the previously placed guide cannula. The length of each infusion cannula was measured to ensure that the distal tip extended ~ 3–4 mm beyond the length of the respective guide. This configuration created a stepped design at the tip of the cannula to maximize fluid distribution during CED procedures. After secure placement of the needle cannula, the animal's head was repositioned in the MR imaging gantry, and CED procedures were initiated while MR imaging data were being continuously acquired. Infusion volumes into each targeted site were between 300 and 700 μl. An initial infusion rate of 0.1 μl/minute was applied and increased at 10-minute intervals to 0.2, 0.5, 0.8, and 1.0 μl/minute, up to 5 μl/minute. Each animal was infused up to 3 times and received liposomal Gd (for survival procedures) or a gadoteridol/rhodamine liposomal mixture (for nonsurvival infusions). The approximate concentration of injected liposomes corresponded to a formulated concentration of 10 mM of phospholipids and 5 mM of gadoteridol. Approximately 15 minutes after infusion, the cannula was withdrawn from the brain. Each animal had at least a 4-week interval between each infusion procedure.

Liposome Infusion in Canines

Four experimental hound/cross dogs (weighing 20–22 kg, with an age of 8 months–3 years) were obtained from Marshall Farms USA, Inc., and 3 clinical dogs (weighing 15–20 kg, with an age of 3–8 years) received liposomal treatment. Experimental protocols were performed in accordance with National Institutes of Health laboratory animal guidelines and the Animal Welfare Act. The experimental protocol was reviewed and approved by the Institutional Animal Care and Use Committee at the University of California, Davis. Experimental dogs were individually housed in concrete runs and maintained on a 12-hour light/dark cycle with a room temperature of 20–22°C. A standard commercial maintenance dry diet was provided on a daily basis with free access to water and chew toys for environmental enrichment. All animals had a complete physical and neurological examination prior to the procedure and were evaluated at various stages of the study.

The infusion cannula system consisted of 4 components: 1) a 22-gauge fused-silica guide cannula molded to a threaded cylindrical plastic pedestal, 2) a 28-gauge fused-silica infusion cannula, 3) a sterile Teflon loading line (0.03-in inner diameter) containing the liposomes, and 4) a nonsterile infusion line containing olive oil. The lengths of the cannulas were determined such that the inner infusion cannula was 2 mm longer than the outer guide cannula, resulting in a step-design. Based on MR imaging coordinates, each guide cannula was mounted onto a stereotactic arm attached to the headframe and was manually guided to the targeted region of the brain through skull bur holes stereotactically placed to reach the target. In each bur hole, a

guide cannula was secured to the skull using brass screws and ultraviolet curing urethane dimethacrylate gel and was sealed prior to infusions by a solid nylon filament dummy cannula. All guide cannulas were left in place for the duration of the study to allow repeated infusions. After infusions, dummy stylets were used to close the guide cannulas and surgical sites. All dogs received intraoperative antibiotics (cefazolin 22 mg/kg, intravenously every 4 hours) and a postoperative 2-week course of oral antibiotics (cephalexin 22 mg/kg, by mouth every 12 hours).

While in a state of general anesthesia, the dogs were affixed to an MR imaging–compatible stereotactic primate headframe modified by the addition of a biteplate holder. Frame components were constructed of Perspex, aluminum, or brass. A dental impression mold was made for each animal in situ by using vinyl polysiloxane impression material putty, and the dogs' heads were stabilized by the biteplate, ear bars, and foam padding placed beneath the rami of the mandibles. Convection-enhanced delivery infusions were performed as previously described.[1] Briefly, dogs were placed in the MR imaging unit, and the infusion cannulas were inserted and secured following attachment of drug-loading and infusion lines. Infusion pressure was generated by a 1-ml syringe loaded with oil and mounted on a microinfusion pump located outside of the MR unit. The initial infusion rate was 0.1 μl/minute, subsequently increased at 10-minute intervals to 0.2, 0.5, 0.8, 1.0, 1.5, 2.0, 2.5 μl/minute, and finally to a maximum of 3.0 μl/minute for ~ 60 minutes. A 300-μl quantity of infusate was delivered over ~ 2.5 hours. Initial infusions were administered in the corona radiata, in the rostral thalamus, or intratumorally with liposomes containing Gd (1.85–3.7 mM) and the chemotherapeutic agent CPT-11 (irinotecan; 48.2 mg/ml) or with liposomes containing Gd alone. Infusions were repeated ~ 4–8 weeks after the first infusion. Animals were reinfused with Gdloaded liposomes or Gd/CPT-11–loaded liposomes.

Magnetic Resonance Imaging Acquisition

The T1-weighted MR images of the primate brains were acquired on a 1.5-T Signa LX scanner (GE Medical Systems) with a 5-in surface coil on the animal's head, parallel to the floor. Prior to insertion of the infusion catheters, baseline spoiled gradient echo images were taken: TR 28 msec, TE 8 msec, flip angle 40°, number of excitations 4, matrix 256 × 192, field of view 16 × 12 cm, and slice thickness 1 mm. These parameters resulted in a 0.391-mm^3 voxel volume. Once the catheters were inserted and the infusion started, spoiled gradient echo scans were taken continuously throughout the infusion. The imaging time was dependent on the number of slices needed to cover the extent of the infusion and ranged from 10 to 12 minutes.

Volume Quantification From MR Images

The volume of liposomal distribution within each infused brain region was quantified on an Apple Macintosh G4 computer with OsiriX Medical Imaging software (version 2.5.1, Apple, Inc.). Magnetic resonance images acquired during the infusion procedure were correlated with the volume of infusion at the start of each series. The OsiriX software reads all data specifications from the MR images. Regions of interest derived from the liposomal gadoteridol signal were manually defined, allowing the software to calculate the area from each coronal MR image and establish the volume of distribution within the brain, which in turn defined the volume of distribution at any given time point during the infusion and allowed 3D image reconstructions.

Results

The infusion of GDL allows us to monitor the progress of CED in vivo with MR imaging. We use this system to track the real-time distribution of therapeutics in various anatomical structures of the central nervous system. In this study we targeted the putamen and corona

radiata in nonhuman primates (Fig. 1A and C) and the thalamus and spontaneously occurring tumors in canines (Fig. 1E and G). Five nonhuman primates received 29 infusions, whereas 7 canines received 25 infusions, for a total of 54 distinct infusions. Ten of these infusions resulted in noticeable leakage into the CSF and accounted for 18.5% of the cases examined. The leaks became evident when areas outside the targeted regions, such as the ventricles (Fig. 1B and D) or sulci (Fig. 1E and H), showed signal enhancement. To determine the effects of liposomal leakage outside the targeted structure during CED, we examined the relationship between the volume distributed versus the volume infused in each case (Fig. 2). The volumes of distribution were calculated by measuring the volume of signal enhancement from coronal MR images acquired during each liposomal infusion session. The volumes infused were quantified by calculating the amount of GDL delivered at the time of each MR imaging series. A review of the graphs shows a plateau after the initial onset of leakage. It is at this point that the change in the volume of distribution decreases sharply, whereas the change in the volume of infusion stays constant, creating a plateau. This pattern indicates that the distribution of liposomes within the brain does not increase further despite continuing infusion of additional material. To quantify this observation, we compared the slope ($\Delta Vd/\Delta Vi$) of these graphs before and after leakage. This slope represents the rate of liposomal distribution within the brain with respect to the volume of material administered. During normal CED procedures, the average slope was 0.0024 (Fig. 3). Instances of liposomal leakage resulted in a 7-fold decrease in the slope, averaging 0.00036. The distribution of GDLs essentially ceases to increase after the onset of leakage. The dramatic decrease in slope occurred during leakage events in all 4 of the structures infused. There was no significant difference in the Vd/Vi between leaks that flowed into the sulci compared with those that emptied into the ventricles.

Discussion

Intraoperative MR imaging is having a significant impact on the practice of neurosurgery, especially in the areas of neurosurgical oncology[8,20,21] and functional neurosurgery.[3,16] The visualization of brain pathology and normal structures by advances in intraoperative imaging can improve overall clinical results and patient safety. Importantly, intraoperative MR imaging can provide realtime visualization of changes in brain anatomy and pathology during surgery, thereby improving the accuracy of neuronavigation. Distinguishing the changes in real time provides a previously unavailable level of confidence for the surgeon.

Convection-enhanced delivery is being applied clinically to treat brain malignancies[12,18] and neurodegenerative disorders, such as Parkinson disease.[5,22] For optimal distribution of therapeutic agents, it is essential to cover the entire targeted treatment area while avoiding other regions of the brain. It has been very difficult to determine the extent of therapeutic delivery by CED and other infusion schemes in real time—both for the delivery of chemotherapeutic agents in neurooncological patients and the administration of growth factors, enzymes, or viral vectors in patients with Parkinson disease. Mixed clinical results have been reported for these delivery techniques in the absence of visual guidance.[9,12]

We have shown that GDLs allow visualization of perfusion via CED in the brain.[10,11,23] Data in the current study suggested that the convected volume is affected by the leakage of material out of brain parenchyma and into the sulci or ventricles. At the onset of leakage the distribution rate of infusate decreases drastically and in many cases stops altogether. This finding is important as it defines the limits of CED through any specific cannula placement. In the event of leakage, altering cannula placement or inserting a second cannula may be necessary to deliver an additional treatment volume. The types of leakage described in this report would not be detectable in the absence of an intraoperative imaging system. Under such circumstances a leak would likely result in failed treatment. Our visualization system ensures accurate cannula

placement and robust delivery of therapeutic agents. Currently, there is no other available modality that allows such close monitoring of in vivo CED infusion.

Neurooncological treatments require pervasive filling of the brain tumor volume with therapeutic agents to achieve optimal results. In cases of spontaneous gliomas in canines, we have significantly ameliorated the clinical course by applying this technique. Similarly, functional neurosurgery requires adequate coverage of the target area—that is, the putamen, subthalamic nucleus, and epileptic focus—by the therapeutic agent for optimal surgical results with CED. So far it has been very difficult to compare clinical results with similar techniques and therapeutic agents given the variability of volume covered by the CED protocol. Although others[24] have proposed possible mechanisms for leakage during CED for brain tumors, we believe that without direct visualization it is impossible to determine whether a treatment failed because of the therapeutic agent's lack of efficacy or because of inadequate delivery and coverage of the targeted area. Utilization of GDLs allows direct visualization that can help standardize treatments, allowing for improved comparisons of similarly treated individuals. More importantly, visualizing leakage on real-time MR imaging allows the physician to discontinue convection, thus minimizing exposure in other regions of the brain.[14]

Conclusions

The use of the surrogate marker GDL during CED treatments in nonhuman primates and canines provided direct, real-time visualization of the perfusion volume. Moreover, MR imaging–documented leakage out of the parenchyma reduced or stopped volume expansion of the CED perfusate. Although mechanisms of leakage continue to be analyzed, this study raises concern regarding the frequency of the leakage phenomenon in the clinical use of CED. We have found that intraoperative GDL–MR imaging procedures can be helpful in the real-time decision making for the neurosurgeon during CED therapy, allowing for better standardization of delivery volumes and simpler comparisons between studies. With the increased application of MR imaging technology in the operating room, the use of strategies similar to ours is likely to improve the results of CED in clinical medicine.

Abbreviations used in this paper

CED, convection-enhanced delivery; CSF, cerebrospinal fluid; DOPC, 1,2-dioleoyl-sn-glycero-3-phosphocholine; GDL, gadoteridol-loaded liposome; HEPES, 4-(2-hydroxyethyl)-1-piperazine ethanesulfonic acid; PEG-DSG, 1,2-distearoyl-sn-glycero-3-[methoxy(polyethylene glycol)-2000.

Acknowledgment

We thank Dr. John Forsayeth of the Department of Neurological Surgery at the University of California, San Francisco, for his editorial assistance.

Disclaimer

This work was supported in part by National Institutes of Health Grant Nos. NS050156-01A2 (National Institute of Neurological Disorders and Stroke) and P50 CA097257 (Specialized Program of Re search Excellence).

References

1. Bankiewicz KS, Eberling JL, Kohutnicka M, Jagust W, Pivirotto P, Bringas J, et al. Convection-enhanced delivery of AAV vector in parkinsonian monkeys; in vivo detection of gene expression and restoration of dopaminergic function using pro-drug approach. Exp Neurol 2000;164:2–14. [PubMed: 10877910]

2. Bobo RH, Laske DW, Akbasak A, Morrison PF, Dedrick RL, Oldfield EH. Convection-enhanced delivery of macromolecules in the brain. Proc Natl Acad Sci U S A 1994;91:2076–2080. [PubMed: 8134351]
3. Chu RM, Tummala RP, Kucharczyk J, Truwit CL, Maxwell RE. Minimally invasive procedures. Interventional MR image-guided functional neurosurgery. Neuroimaging Clin N Am 2001;11:715–725. [PubMed: 11995426]
4. Cunningham J, Oiwa Y, Nagy D, Podsakoff G, Colosi P, Bankiewicz KS. Distribution of AAV-TK following intracranial convection-enhanced delivery into rats. Cell Transplant 2000;9:585–594. [PubMed: 11144956]
5. Gill SS, Patel NK, Hotton GR, O'Sullivan K, McCarter R, Bunnage M, et al. Direct brain infusion of glial cell line-derived neurotrophic factor in Parkinson disease. Nat Med 2003;9:589–595. [PubMed: 12669033]
6. Hadaczek P, Yamashita Y, Mirek H, Tamas L, Bohn MC, Noble C, et al. The "perivascular pump" driven by arterial pulsation is a powerful mechanism for the distribution of therapeutic molecules within the brain. Mol Ther 2006;14:69–78. [PubMed: 16650807]
7. Hsieh CH, Chen YF, Chen FD, Hwang JJ, Chen JC, Liu RS, et al. Evaluation of pharmacokinetics of 4-borono-2-(18)F-fluoro-L-phenylalanine for boron neutron capture therapy in a glioma-bearing rat model with hyperosmolar blood-brain barrier disruption. J Nucl Med 2005;46:1858–1865. [PubMed: 16269600]
8. Hunt MA, Bago AG, Neuwelt EA. Single-dose contrast agent for intraoperative MR imaging of intrinsic brain tumors by using ferumoxtran-10. AJNR Am J Neuroradiol 2005;26:1084–1088. [PubMed: 15891164]
9. Kordower JH, Palfi S, Chen EY, Ma SY, Sendera T, Cochran EJ, et al. Clinicopathological findings following intraventricular glial-derived neurotrophic factor treatment in a patient with Parkinson's disease. Ann Neurol 1999;46:419–424. [PubMed: 10482276]
10. Krauze MT, Forsayeth J, Park JW, Bankiewicz KS. Real-time imaging and quantification of brain delivery of liposomes. Pharm Res 2006;23:2493–2504. [PubMed: 16972184]
11. Krauze MT, McKnight TR, Yamashita Y, Bringas J, Noble CO, Saito R, et al. Real-time visualization and characterization of liposomal delivery into the monkey brain by magnetic resonance imaging. Brain Res Brain Res Protoc 2005;16:20–26. [PubMed: 16181805]
12. Kunwar S. Convection enhanced delivery of IL13-PE38QQR for treatment of recurrent malignant glioma: presentation of interim findings from ongoing phase 1 studies. Acta Neurochir Suppl 2003;88:105–111. [PubMed: 14531568]
13. Kunwar S, Prados MD, Chang SM, Berger MS, Lang FF, Piepmeier JM, et al. Direct intracerebral delivery of cintredekin besudotox (IL13-PE38QQR) in recurrent malignant glioma: a report by the Cintredekin Besudotox Intraparenchymal Study Group. J Clin Oncol 2007;25:837–844. [PubMed: 17327604]
14. Lidar Z, Mardor Y, Jonas T, Pfeffer R, Faibel M, Nass D, et al. Convection-enhanced delivery of paclitaxel for the treatment of recurrent malignant glioma: a phase I/II clinical study. J Neurosurg 2004;100:472–479. [PubMed: 15035283]
15. Lieberman DM, Laske DW, Morrison PF, Bankiewicz KS, Oldfield EH. Convection-enhanced distribution of large molecules in gray matter during interstitial drug infusion. J Neurosurg 1995;82:1021–1029. [PubMed: 7539062]
16. Liu H, Hall WA, Truwit CL. The roles of functional MRI in MR-guided neurosurgery in a combined 1.5 Tesla MR-operating room. Acta Neurochir Suppl 2003;85:127–135. [PubMed: 12570148]
17. Mardor Y, Rahav O, Zauberman Y, Lidar Z, Ocherashvilli A, Daniels D, et al. Convection-enhanced drug delivery: increased efficacy and magnetic resonance image monitoring. Cancer Res 2005;65:6858–6863. [PubMed: 16061669]
18. Mardor Y, Roth Y, Lidar Z, Jonas T, Pfeffer R, Maier SE, et al. Monitoring response to convection-enhanced taxol delivery in brain tumor patients using diffusion-weighted magnetic resonance imaging. Cancer Res 2001;61:4971–4973. [PubMed: 11431326]
19. Nguyen JB, Sanchez-Pernaute R, Cunningham J, Bankiewicz KS. Convection-enhanced delivery of AAV-2 combined with heparin increases TK gene transfer in the rat brain. Neuroreport 2001;12:1961–1964. [PubMed: 11435930]

20. Nimsky C, Ganslandt O, von Keller B, Fahlbusch R. Intraoperative high-field MRI: anatomical and functional imaging. Acta Neurochir Suppl 2006;98:87–95. [PubMed: 17009705]

21. Nimsky C, Ganslandt O, von Keller B, Fahlbusch R. Preliminary experience in glioma surgery with intraoperative high-field MRI. Acta Neurochir Suppl 2003;88:21–29. [PubMed: 14531557]

22. Patel NK, Bunnage M, Plaha P, Svendsen CN, Heywood P, Gill SS. Intraputamenal infusion of glial cell line-derived neurotrophic factor in PD: a two-year outcome study. Ann Neurol 2005;57:298–302. [PubMed: 15668979]

23. Saito R, Krauze MT, Bringas JR, Noble C, McKnight TR, Jackson P, et al. Gadolinium-loaded liposomes allow for real-time magnetic resonance imaging of convection-enhanced delivery in the primate brain. Exp Neurol 2005;196:381–389. [PubMed: 16197944]

24. Sampson JH, Brady ML, Petry NA, Croteau D, Friedman AH, Friedman HS, et al. Intracerebral infusate distribution by convection-enhanced delivery in humans with malignant gliomas: descriptive effects of target anatomy and catheter positioning. Neurosurgery 2007;60(2 Suppl):ONS89–ONS99. [PubMed: 17297371]

25. Sampson JH, Raghavan R, Brady ML, Provenzale JM, Herndon JE II, Croteau D, et al. Clinical utility of a patient-specific algorithm for simulating intracerebral drug infusions. Neuro Oncol 2007;9:343–353. [PubMed: 17435179]

26. Weyerbrock A, Walbridge S, Pluta RM, Saavedra JE, Keefer LK, Oldfield EH. Selective opening of the blood-tumor barrier by a nitric oxide donor and long-term survival in rats with C6 gliomas. J Neurosurg 2003;99:728–737. [PubMed: 14567609]

27. Zhang Y, Pardridge WM. Delivery of beta-galactosidase to mouse brain via the blood-brain barrier transferrin receptor. J Pharmacol Exp Ther 2005;313:1075–1081. [PubMed: 15718287]

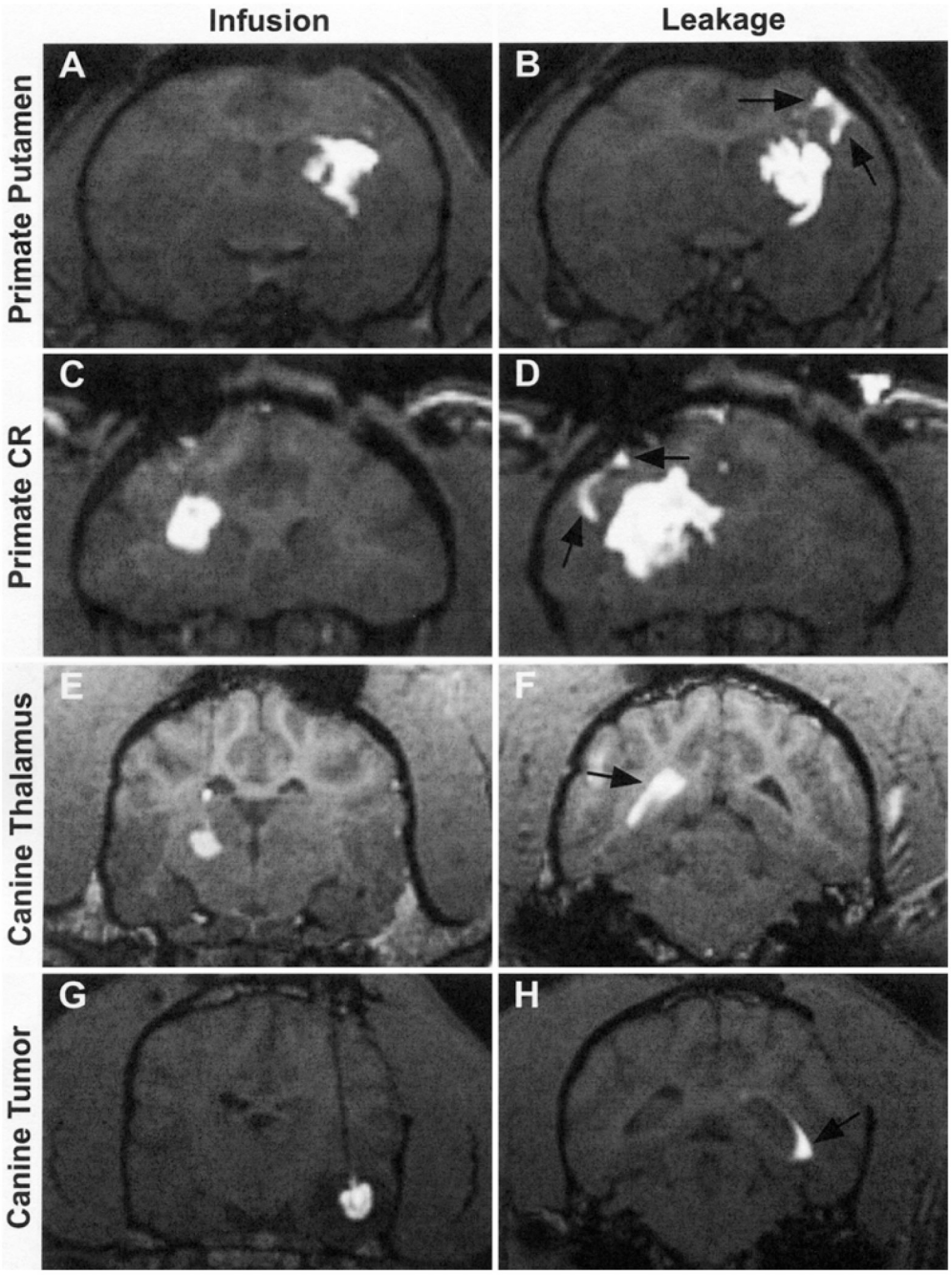

FIG. 1.

Coronal MR images showing the CED distribution of gadoteridol liposomes in 4 specific sites and the leakages associated with each infusion. A and B: Primate putamen infusion and corresponding sulcal leakage. C and D: Primate corona radiata infusion and corresponding sulcal leakage. E and F: Canine thalamus infusion and corresponding ventricular leakage. G and H: Canine tumor infusion and corresponding ventricular leakage.

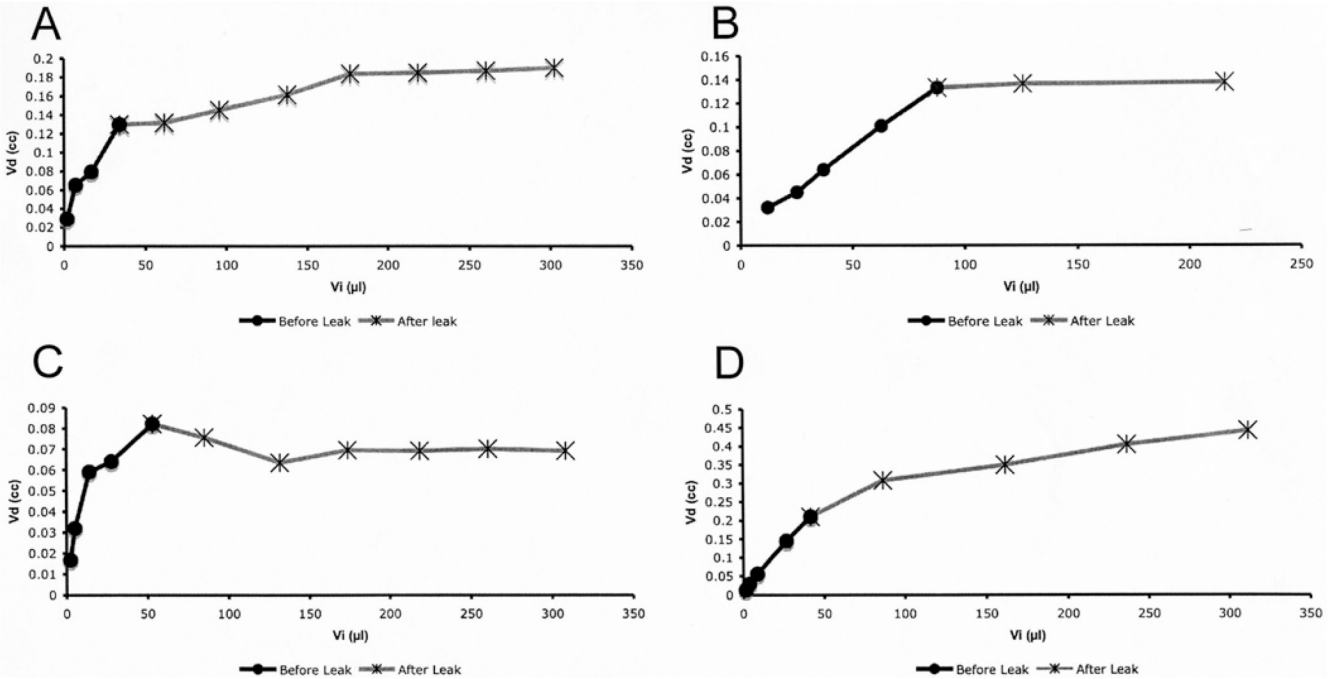

FIG. 2.

Graphs depicting the volume distributed (Vd) versus the volume infused (Vi) of 4 infusions that resulted in liposomal leakage. A: Primate putamen infusion. B: Primate corona radiata infusion. C: Canine thalamus infusion. D: Canine tumor infusion.

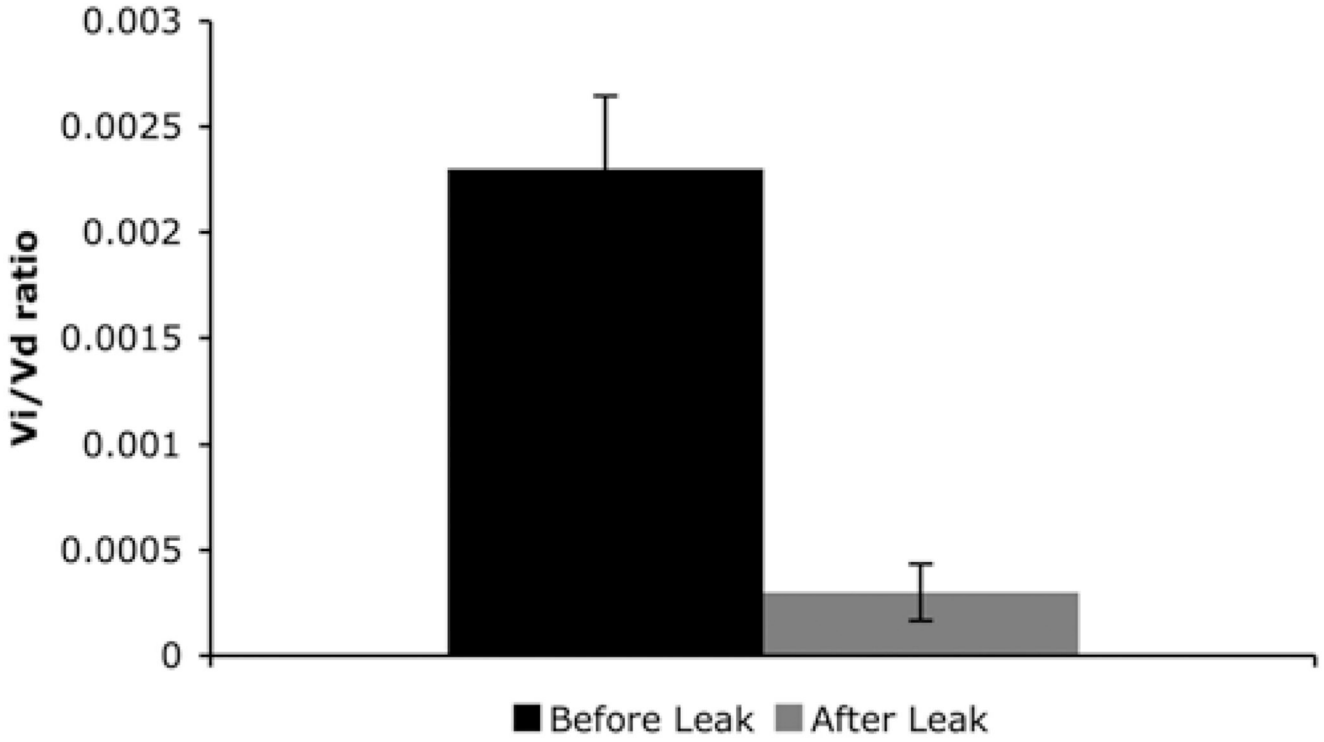

FIG. 3.
Bar graph showing a comparison of the average slope (ΔVd/ΔVi) before and after leakage from 10 liposomal infusion cases. Standard error bars are shown.